Journal of Electronic Materials, Vol. 21, No. 1, 1992

Formation of Titanium and Cobalt Germanides on Si (100) Using Rapid Thermal Processing

S. P. ASHBURN, M. C. ÖZTÜRK and J. J. WORTMAN

Department of Electrical & Computer Engineering
North Carolina State University, Raleigh, NC 27695-7911

G. HARRIS, J. HONEYCUTT and D. M. MAHER

Department of Materials Science and Engineering
North Carolina State University, Raleigh, NC 27695-7911

Titanium and cobalt germanides have been formed on Si (100) substrates using rapid thermal processing. Germanium was deposited by rapid thermal chemical vapor deposition prior to metal evaporation. Solid phase reactions were then performed using rapid thermal annealing in either Ar or N_2 ambients. Germanide formation has been found to occur in a manner similar to the formation of corresponding silicides. The sheet resistance was found to be dependent on annealing ambient (Ar or N_2) for titanium germanide formation, but not for cobalt germanide formation. The resistivities of titanium and cobalt germanides were found to be 20 $\mu\Omega$-cm and 35.3 $\mu\Omega$-cm, corresponding to $TiGe_2$ and Co_2Ge, respectively. During solid phase reactions of Ti with Ge, we have found that the Ti_6Ge_5 phase forms prior to $TiGe_2$. The $TiGe_2$ phase was found to form approximately at 800° C. Cobalt germanide formation was found to occur at relatively low temperatures (425° C); however, the stability of the material is poor at elevated temperatures.

Key words: Germanide, silicide, germanium, silicon, titanium, cobalt, RTCVD, RTA, LPCVD, CVD

1. INTRODUCTION

Metal silicides are currently used in very-large-scale integration technologies for low resistivity interconnect lines and contacts to silicon substrates. The use of Ge and Ge/Si alloys is currently under investigation for applications in advanced silicon based device structures. Optimal implementation of these device technologies will require an understanding of reactions occurring between metals and Ge or Ge/Si alloys. Germanide formation, however, has received far less attention than the formation of silicides.[1–3] In addition, the results on germanide formation to date have been obtained by furnace annealing. It is well known that titanium and cobalt have a tendency to easily form oxides. Titanium can easily form nitrides as well, and therefore, when using conventional furnace annealing to form silicides, care must be taken to avoid the effects of impurities (O_2, N_2). Rapid thermal processing (RTP), however, is a growing technology which has found many applications in silicon processing including the formation of silicides.[4–8] The use of RTP for silicide formation has been shown to be quite effective for producing oxide-free and homogeneous silicidation of Ti films on Si as well as for Co films on Si.[9,10] In this work we have studied the solid phase formation of titanium and cobalt germanides using rapid thermal annealing (RTA). Characterization of the germanides formed by RTA was performed using four-point-probe sheet resistance measurements, Auger electron spectroscopy (AES), cross-sectional transmission electron microscopy (XTEM), Rutherford backscattering spectroscopy (RBS), and x-ray diffraction analysis.

2. EXPERIMENTAL

The substrates used in this study were 4-inch, *n*-type, silicon wafers of (100) orientation. The resistivities of the substrates were between 0.2 and 0.45 Ω-cm. Upon completion of an RCA clean, 150 nm of Ge was deposited onto the wafers by rapid thermal chemical vapor deposition. Germanium depositions were performed in a LEISK™ rapid thermal processor. A cross-sectional view of the system is shown in Fig. 1. In this system, heating of the wafer is provided by two banks of tungsten-halogen lamps with the lamps oriented at 90° to each other to reduce temperature gradients across the substrate. The temperature is monitored by a pyrometer (λ = 3.5–4.1 μm) focused on the back center of the wafer. The depositions were accomplished using the thermal decomposition of GeH_4 premixed with H_2. A pressure and temperature of 3 Torr and 450° C, respectively, were used. The details of the deposition conditions and structural characterization of the films can be found elsewhere.[11] Following Ge depositions, 50 nm of Ti or 30 nm of Co was evaporated onto the substrates in a conventional evaporator utilizing

(Received September 4, 1991; revised October 16, 1991)

0361-5235/1992/1401-081$5.00©92 TMS

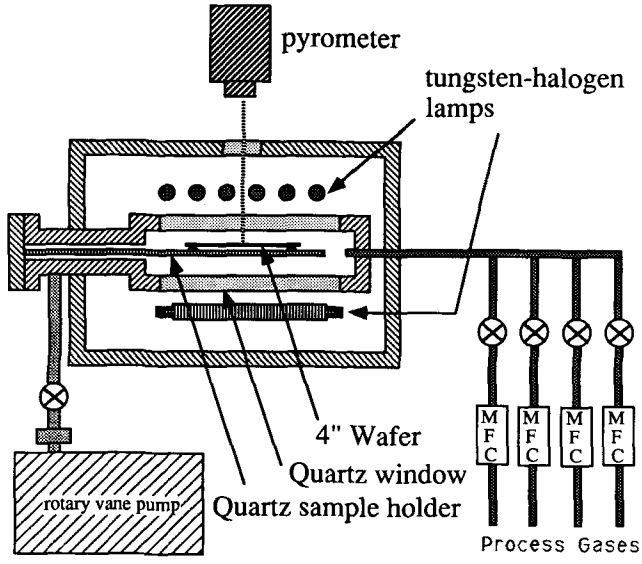

Fig. 1 — Cross-sectional view of LEISK™ rapid thermal processing system.

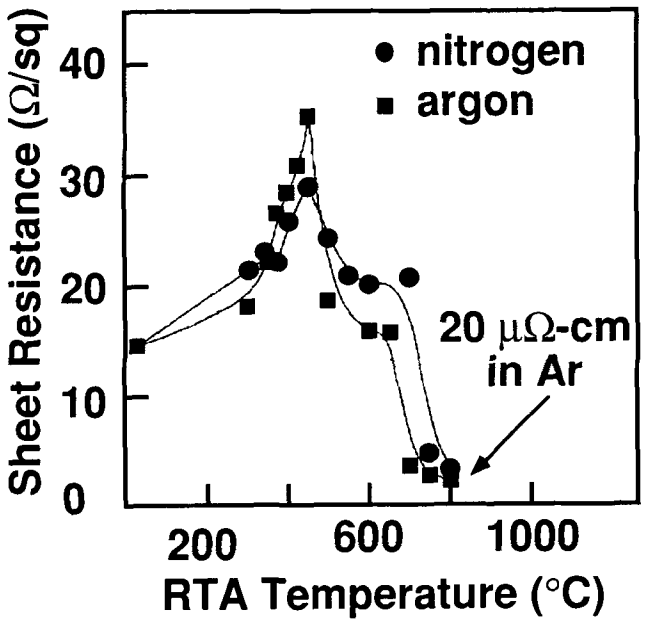

Fig. 2 — Sheet resistance of 50 nm Ti/150 nm Ge after 10 sec RTA in Ar and N_2 ambients.

resistive heating. Annealing of the samples was carried out in an AG Associates™ Heatpulse 210T Rapid Thermal Annealer at atmospheric pressure in either Ar or N_2 ambients. The chamber was purged for three min with the annealing ambient gas prior to RTA. The LEISK system is used primarily for Ge and Ge/Si depositions. The vacuum capability of this system, in comparison to the atmospheric operation of the Heatpulse, would decrease the effect of impurities on the germanide formation during RTA. However, metals are not put in this system in order to avoid contamination.

3. EXPERIMENTAL RESULTS

The temperature dependence of the sheet resistance of titanium germanide formed by RTA in both Ar and N_2 ambients is shown in Fig. 2. As shown, an initial increase in sheet resistance occurs, reaching a maximum in both ambients at 450° C. Sheet resistance values at this temperature were determined to be 35.3 Ω/sq and 29.1 Ω/sq in Ar and N_2 RTA ambients, respectively. Between 600 and 700° C there is a rapid decrease in sheet resistance to a minimum value of 2.1 Ω/sq in Ar and 3.1 Ω/sq in N_2 at 800° C. Higher sheet resistance values have also been observed for $TiSi_2$ formed in a N_2 ambient using RTA.[10,12] Using the germanide thickness values obtained from Auger electron spectroscopy (AES) and transmission electron microscopy (TEM), the resistivity of titanium germanide was determined to be 20 $\mu\Omega$-cm after an 800° C RTA.

The increase in sheet resistance from 300° C to a maximum occuring at 450° C can be partially explained by observing the AES depth profiles of Fig. 3. As shown in Fig. 3a, a small layer of oxygen exists on the Ti surface prior to RTA. This surface oxide is believed to occur during the transfer of the substrates from the metal evaporator to the RTA system. Figure 3b shows that during RTA in an Ar ambient, the oxygen diffuses into the Ti layer reaching an equidistribution at 450° C. We have also observed this oxygen redistribution for films annealed in a N_2 ambient. Similar phenomena have also been observed during the formation of $TiSi_2$, and the increase in sheet resistance has been attributed primarily to oxygen incorporation into the metal.[10]

We have used x-ray diffraction analysis with Cu Kα radiation to study phase formation and phase transitions occuring during germanide formation. The technique can be used to identify the existing phases, however, it can not provide relative concentrations of phases present in the film. The results are shown in Fig. 4. As shown in Fig. 4a, the titanium germanide phase formed after a 425° C, 10 sec RTA, corresponds to Ti_6Ge_5 ($\rho \approx 150$ $\mu\Omega$-cm). Upon higher RTA temperatures (650–800° C), a phase transition to the low resistivity (20 $\mu\Omega$-cm) $TiGe_2$ (C54) phase occurs. This is demonstrated in Fig. 4b for a sample annealed at 800° C. Therefore, differences in resistivities obtained at different RTA temperatures may also be related to different crystalline structures of these two phases. A more detailed study of the phase sequence occurring during $TiGe_2$ formation is currently being investigated.

It is interesting to note that a Ti_6Ge_5 (002) peak also exists after RTA at 800° C as shown in Figure 4b. This peak may be attributed to the incomplete transformation of a thin (≈100Å) Ti_6Ge_5 layer on the surface of the sample to $TiGe_2$. Figure 5, which shows a cross-sectional transmission electron micrograph of the Ti/Ge/Si stacked structure after a 750° C, 10 sec RTA, is also suggestive of two clearly distinguishable grain structures. Using the microprobe diffraction analysis capability of the TEM system, we have found that the large grains shown

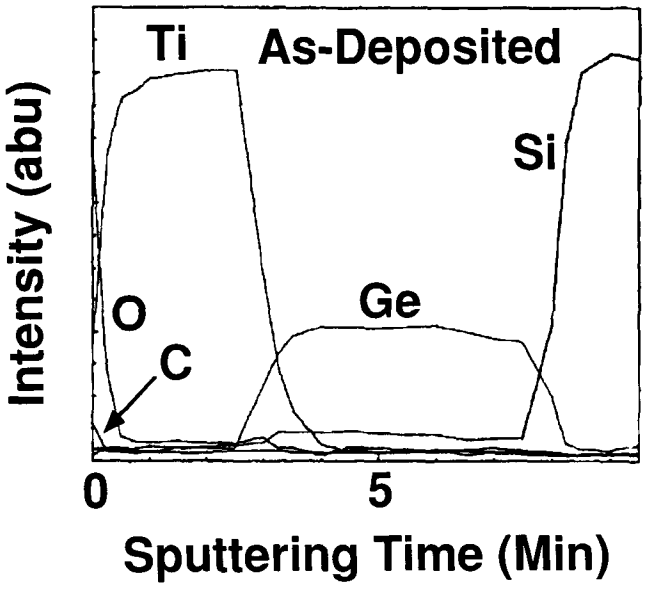

(a)

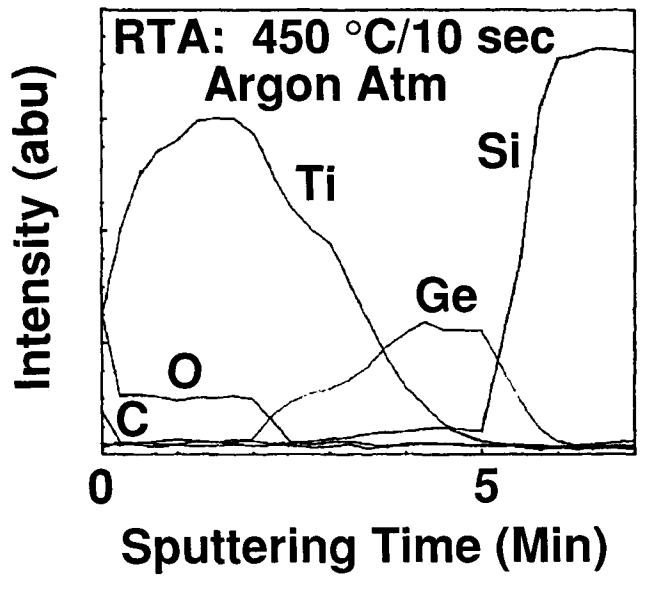

(b)

Fig. 3 — AES depth profiles of a) as-deposited Ti/Ge/Si stacked structure and b) after 10 sec/450° C RTA in Ar, demonstrating the oxygen redistribution in the Ti layer.

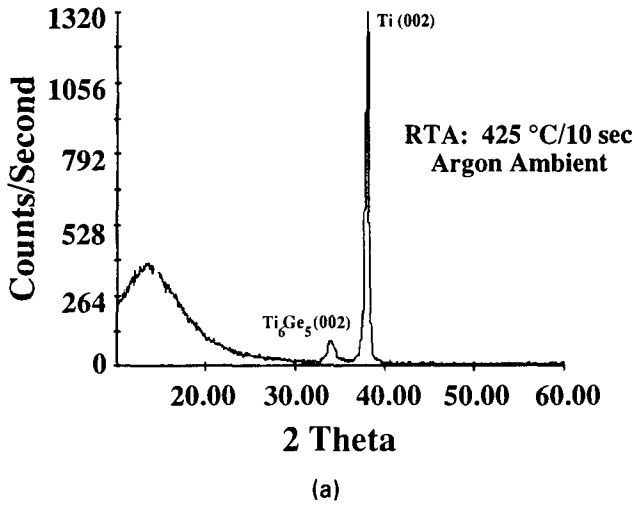

(a)

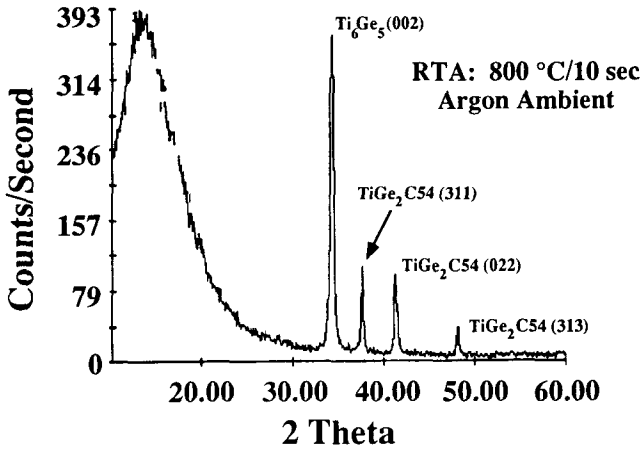

(b)

Fig. 4 — Partial diffraction patterns showing the formation of a) high resistivity (≈150 $\mu\Omega$-cm) Ti_6Ge_5 and b) low resistivity (≈20 $\mu\Omega$-cm) $TiGe_2$ at different RTA temperatures.

in Fig. 5 correspond to $TiGe_2$. The small grain structures on the surface of the sample are thus believed to be contributing to the Ti_6Ge_5 peak observed with x-ray diffraction analysis.

During rapid thermal chemical vapor deposition of the Ge layer, strain occurs in the Ge layer due to the lattice mismatch (4.2%) between the Ge and un-

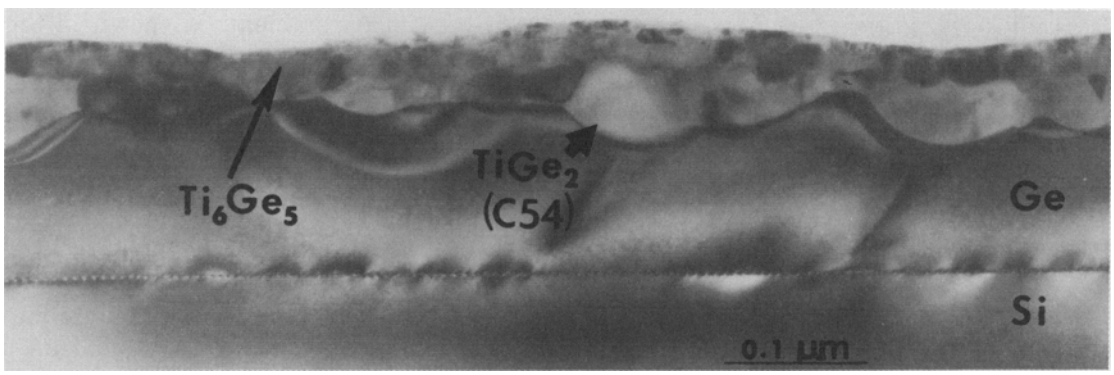

Fig. 5 — Cross-sectional transmission electron micrograph of the Ti/Ge/Si stacked structure after a 750° C/10 sec RTA in Ar.

derlying Si substrate. Figure 5 shows that after a 750° C, 10 sec RTA, the strain in the Ge layer is completely relieved. This strain relaxation occurs by the formation of misfit dislocations at the Ge/Si interface and threading dislocations in the Ge layer. These threading dislocations may extend completely through the Ge layer terminating at the $TiGe_2$/Ge interface as can be seen in Fig. 5. Also, observed in Fig. 5, is that the Ge layer has not been entirely consumed after the 750° C, 10 sec RTA cycle. Auger electron spectroscopy depth profiles and TEM cross-sections have been used to determine the Ge consumption which occurs during $TiGe_2$ formation. We have found that the Ge:Ti consumption ratio is approximately 2.5. This ratio is very close to the Si:Ti consumption ratio for $TiSi_2$ formation (Si:Ti = 2.3).

Figure 6 shows the AES depth profiles for samples annealed in N_2 and Ar ambients at 800 and 750° C, respectively. As shown, during high temperature RTA, the oxygen on the metal surface is not incorporated in the germanide resulting in an oxygen peak at the surface of the sample. Evidence of similar effects has been observed in the formation of $TiSi_2$, and this behavior has been attributed to the inability of the oxygen to redistribute into the unreacted titanium layer as rapidly as the silicide growth front consumes the titanium.[13]

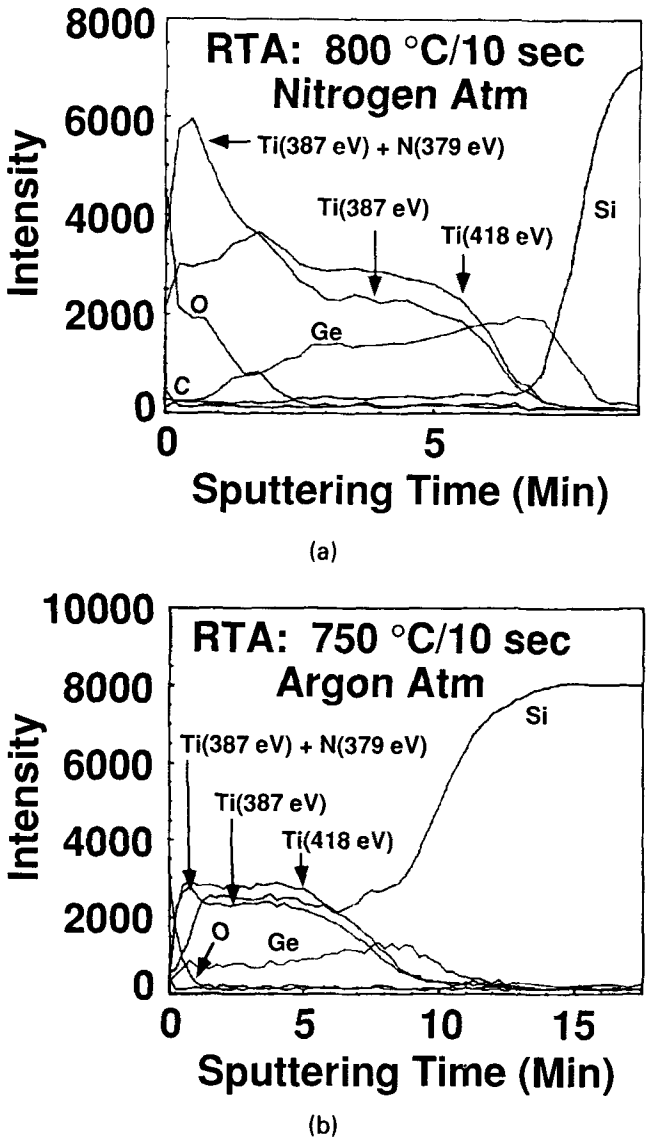

Fig. 6 — AES depth profiles of a) 800° C/10 sec RTA in N_2 and b) 750° C/10 sec RTA in Ar, demonstrating the effects of annealing ambient on germanide formation.

Another interesting observation that can be obtained from Fig. 2 is that the sheet resistance of the samples annealed in N_2 at temperatures above 450° C is higher than the sheet resistance of the samples annealed in Ar. This may be attributed to the formation of TiN (as determined by Rutherford backscattering spectroscopy) on the surface of the Ti layer and also to the possibility that the germanide may contain some dissolved nitrogen, or one or more titanium nitride phases.

We have also used AES to investigate the formation of a titanium nitride layer at the sample surface during RTA in a N_2 ambient. Titanium has two Auger energy peaks occurring at 387 eV and 418 eV. Quantitative AES analysis is difficult for titanium nitride, because the principle nitrogen Auger peak ($KL_{23}L_{23}$) at 379 eV overlaps with the $L_3M_{23}M_{23}$ Ti Auger peak at 387 eV.[14,15] Therefore, when analyzing films which contain both Ti and N, one must be very careful of the overlap which can occur between these nitrogen and Ti peaks. For a pure Ti layer, the two Ti signals (Ti 387 eV and Ti 418 eV) should follow each other with a fixed ratio of 0.8 in the AES depth profiles with the Ti 418 eV signal above the Ti 387 eV signal. Therefore, any deviation from a fixed ratio can be taken as the indication of the presence of a titanium oxide, a titanium nitride or both. This is clearly observed at the surface of the sample shown in Fig. 6a. It is also observed that the N (379 eV) plus Ti (387 eV) signal at the surface has an intensity approximately 2.13 times the intensity of the Ti (418 eV) signal. This ratio of intensities is indicative of the presence of a TiN layer. It is also observed that a nitrogen signal is present at the surface of the sample annealed in Ar. This is shown in Figure 6b. However, the ratio of intensities between the Ti (387 eV) + N(379 eV) signal to the Ti(418 eV) signal is much less for the sample annealed in Ar than the one annealed in N_2.

The temperature dependence of sheet resistance for the formation of cobalt germanide annealed in both N_2 and Ar ambients is shown in Fig. 7. The resistivity increases from an as deposited value of 17.1 $\mu\Omega$-cm to a maximum at around approximately 300° C in both Ar and N_2 ambients. The differences occurring in sheet resistance values around 300° C is being investigated. It is possible that the peak sheet resistance in a nitrogen ambient is achieved at a slightly lower temperature than the minimum temperature capability of the annealer used in this work. At temperatures above 300° C there is a sharp decrease in sheet resistance to a minimum value corresponding to a resistivity of 35.3 $\mu\Omega$-cm. This minimum value occurs at a temperature of 425° C which is considerably lower than that reported for

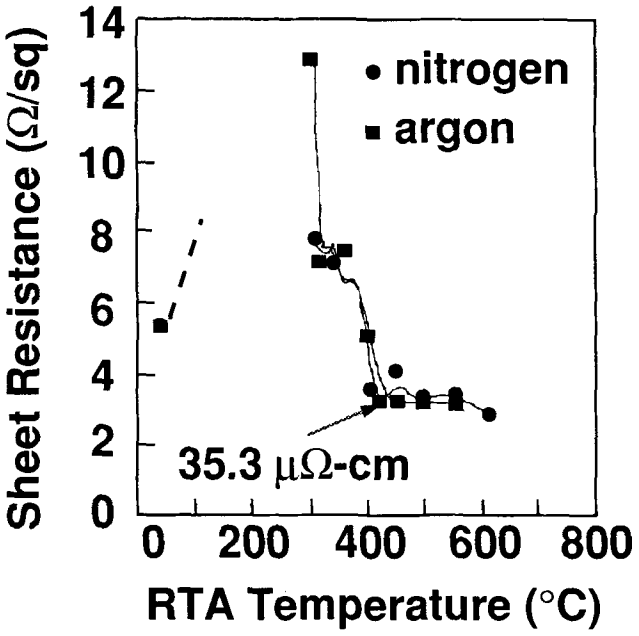

Fig. 7 — Sheet resistance of 30 nm Co/150 nm Ge after 10 sec RTA in Ar and N_2 ambients.

cobalt silicide which occurs at approximately 700° C. A study of the phases forming during the cobalt germanide reaction process is being investigated. However, we have found using microprobe diffraction analysis that the low resistivity cobalt germanide phase occurring after a 475° C, 10 sec RTA corresponds to Co_2Ge. Figure 7 also shows that the nitrogen ambient has little if any effect on the sheet resistance at temperatures above 300° C. This may be attributed to the very low solid solubility of N_2 in Co.[16] As shown in Fig. 8, nitrogen was not incorporated into the material during RTA. Similar to the formation of $TiSi_2$, there is no oxygen incorporation in the germanide around the low resistivity region.

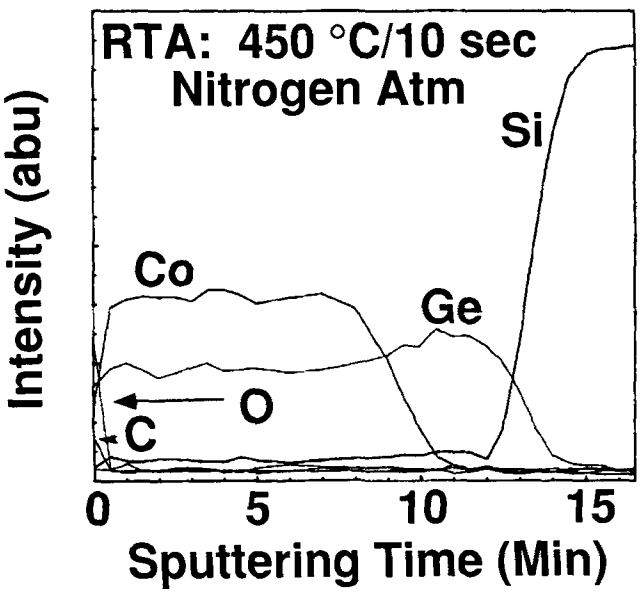

Fig. 8 — AES depth profile of Co/Ge/Si stacked structure after 425° C/10 sec RTA in N_2.

We have found using TEM and AES analysis that the stability of the cobalt germanide reaction process is poor at elevated temperatures. These measurements indicate that Ge begins to diffuse through the germanide layer and agglomerate on the surface at tempertures in excess of 700° C. In some cases, we have observed complete penetration of the germanium layer by Co which then produces the formation of an underlying $CoSi_2$. The reason for this instability is currently under investigation. However, we believe that the stability is strongly related to the crystalline quality of the Ge layer.

4. CONCLUSIONS

In summary, we have formed titanium and cobalt germanides on Si (100) substrates using RTP. Solid phase reactions were performed using rapid thermal annealing in both Ar and N_2 ambients. Nitrogen annealing ambients have been shown to increase the sheet resistance of titanium germanide formation possibly due to the formation of TiN on the surface of the substrate and also due to the possibility of the titanium germanide containing one or more titanium nitride phases. The phase formation and transitions occurring during germanide formation are being investigated. However, we have found that the high resistivity Ti_6Ge_5 phase preceeds the final low resistivity $TiGe_2$ (C54) phase. We have determined that the Ge:Ti consumption ratio is approximately 2.5. The formation of cobalt germanide is not affected by the annealing ambient (Ar or N_2) which may be attributed to the low solid solubility of N_2 in Co. The titanium germanide resistivity was determined to be 20 $\mu\Omega$-cm using an 800° C RTA cycle. A resistivity of 35.3 $\mu\Omega$-cm has been obtained for the cobalt germanide materials for RTA at temperatures of 400–600° C.

ACKNOWLEDGMENTS

This work has been partially supported by the NSF Engineering Research Centers Program through the Center for Advanced Electronic Materials Processing (Grant CDR-8721505) and SRC Microstructures Sciences Program (Grant 90-SJ-081). The authors also greatly appreciate the work of S. Hofmeister (NCSU) for AES analysis, John Clarke (MCNC) for metal evaporation and J. O'Sullivan and R. Kuehn (NCSU) for assisting with many of the processing steps leading to these results.

REFERENCES

1. O. Thomas, F. M. d'Heurle and S. Delage, J. Mater. Res. V *5*, 1453 (1990).
2. Q. Z. Hong, J. G. Zhu, C. B. Carter and J. W. Mayer, Appl. Phys. Lett. *58*, 905 (1991).

3. E. D. Marshall, C. S. Wu, C. S. Pai, D. M. Scott and S. S. Lau, Mater. Res. Soc. Symp. Proc. *47,* 161 (1985).
4. P. Vandenabeele and K. Maex, Microelectronic Eng. *10,* 207 (1991).
5. R. A. Powell, R. Chow, C. Thridandam, R. T. Fulks, I. A. Blech and J. D. T. Pan, IEEE Electron Device Lett. Vol. *EDL-4(10),* 380 (1983).
6. T. Yachi, IEEE Electron Device Lett. *EDL-5,* 217 (1984).
7. M. Tabasky, E. S. Bulat, B. M. Ditchek, M. A. Sullivan and S. Shatas, Mater. Res. Soc. Proc., Pittsburgh, *52,* 271 (1985).
8. S. Leavitt, Semicond. Int., March (1987).
9. T. Okamoto, K. Tsukamoto, M. Shimizu and T. Matsukawa, J. Appl. Phys. *57,* 5251 (1985).
10. L. Van Den Hove, Ph.D. diss., Kathulieke Universiteit Leuven, Belgium (1988).
11. M. C. Öztürk, D. T. Grider, J. J. Wortman, M. A. Littlejohn and Y. Zhong, J. Electron. Mater. *19,* 1129 (1990).
12. P. J. Rosser and G. J. Tomkins, Mater. Res. Soc. Symp. Proc. *35,* 457 (1985).
13. P. Merchant and J. Amano, J. Vac. Sci. Technol. *B2,* 762 (1984).
14. N. Biunno, J. Narayan, S. K. Hofmeister, A. R. Srivatsa and R. K. Singh, Appl. Phys. Lett. Vol. (1989).
15. S. Hofmann, J. Vac. Sci. Technol. *A4,* 2789 (1986).
16. L. Gmelin, Handbook of Inorganic Chemistry, Cobalt, Chemie, Weinheim, Germany, Vol. *A,* 511 (1961).